

Femtosecond quasiparticle relaxation dynamics and probe polarization anisotropy in $\text{YSr}_x\text{Ba}_{2-x}\text{Cu}_4\text{O}_8$ ($x=0,0.4$)

D. Dvorsek,¹ V. V. Kabanov,¹ J. Demsar,^{1,2} S. M. Kazakov,³ J. Karpinski,³ and D. Mihailovic¹

¹*Jozef Stefan Institute, Jamova 39, 1000 Ljubljana, Slovenia*

²*Los Alamos National Laboratory, Los Alamos, New Mexico 87545*

³*Institut für Festkörperphysik, ETH Zurich, Switzerland*

(Received 24 January 2002; published 24 July 2002)

Femtosecond pump probe experiments are reported on quasiparticle relaxation and recombination in $\text{YSr}_x\text{Ba}_{2-x}\text{Cu}_4\text{O}_8$ as a function of temperature and polarization. The data show a two-component relaxation similar to $\text{YBa}_2\text{Cu}_3\text{O}_{7-\delta}$, one component being associated with the superconducting transition, and the other with the pseudogap below T^* . The relaxation time τ_p associated with the pseudogap is found to be T independent, while the relaxation time τ_G of the component observed only below T_c exhibits a clear divergence near T_c . A strong polarization anisotropy of the picosecond transient is observed below T_c which is attributed to the anisotropy of the probe transition matrix elements.

DOI: 10.1103/PhysRevB.66.020510

PACS number(s): 74.72.-h, 78.47.+p

Femtosecond time-domain spectroscopy is capable of giving important information on the quasiparticle excitations and a low-energy structure of correlated electron systems, and particularly high- T_c superconducting cuprates (HTSC). Measurements on $\text{YBa}_2\text{Cu}_3\text{O}_{7-\delta}$ (Y123) at different doping levels have shown two-component relaxation dynamics on the picosecond time scale, that was attributed to the simultaneous existence of two gaps in optimally doped and overdoped regions.¹ Moreover, similar two-component relaxation dynamics has been thus far observed in several HTSC,²⁻⁸ suggesting this being a general feature in these materials. The magnitude and sign of the two components at temperatures below T_c were found to depend on the material, probe wavelength,⁹ and also the effects of probe polarization dependence were investigated on untwinned Y123 single crystals,¹⁰ where a response parallel and perpendicular to the Cu-O chains was separately probed and found to be different. In some cases (Tl2201², Bi2212³) the signs of the different components observed in the relaxation were opposite. However, the anisotropy of the photoinduced signal with respect to the probe pulse polarization has not been discussed in detail thus far.

The purpose of this paper is twofold. First, we show that the two-component relaxation behavior observed in Y123 is similar also in $\text{YBa}_2\text{Cu}_4\text{O}_8$ (Y124), and second, utilizing the fact that Y124 has a fixed oxygen content and a well-defined untwinned orthorhombic structure, to probe the polarization dependence of the photoinduced signal.

We report on a systematic investigation of Y124 and $\text{YBa}_{1.6}\text{Sr}_{0.4}\text{Cu}_4\text{O}_8$ (Y124:Sr) using the usual femtosecond time-resolved pump-probe technique. As discussed in detail previously,¹¹ a short (~ 80 fs) pump laser pulse excites the carriers in the sample. Photoexcited electrons and holes with energies on the order of photon energy quickly thermalize via electron-electron and electron-phonon thermalization, reaching states just above the gap in a time short compared to the pulse duration. The gap in the density of states presents a relaxation bottleneck, and the relaxation of photoexcited carrier density near E_F is measured through measure-

ment of small changes in the optical reflectivity $\Delta R/R$ or transmittance $\Delta T/T$ of the sample as a function of a time delay between the pump and probe pulses. In these experiments, a Ti:sapphire mode-locked laser, which operated at a 78 MHz repetition rate, was used as a source of both pump and probe light pulses. The wavelength of the pulses was centered at approximately $\lambda \approx 800$ nm (1.58 eV) and the intensity ratio of pump and probe pulses was $\approx 100:1$. The pump and probe beams were crossed on the sample's surface, where the angle of incidence of both beams was less than 10° . The diameter of both beams on the surface was ~ 100 μm and the surface was parallel to a ab -crystal plane. The typical energy of pump pulses was 0.2 nJ (1.25×10^9 eV), which produces a weak perturbation of the electronic system with $\approx 3 \times 10^{10}$ thermalized photoexcited carriers per pulse. (The approximation is based on the assumption that each photon creates $\hbar\omega/\Delta$ thermalized photoexcited carriers, where $\Delta \approx 40$ meV is of the order of the superconducting gap.) The train of the pump pulses was modulated at 200 kHz with an acousto-optic modulator and the small optical changes were resolved out of noise with the aid of phase-sensitive detection using EG&G digital lock-in amplifier model 7265. The pump and probe beams were also cross polarized to reduce scattering of pump beam into the detector (avalanche photodiode). A detailed description of the experimental technique and the theory of excitation and relaxation of the photoexcited carriers in superconductors with different gap structures can be found in Refs. 11 and 12.

The two Y124 samples used for this investigation were prepared in Zürich by a nonstoichiometric flux-growth technique, using a BaO-CuO eutectic mixture as the flux. In the Sr-doped compound, part of the Ba was substituted with Sr. The crystals grew at a pressure of 900 bars and temperatures of 1000 °C to 1120 °C. So obtained crystals had a thickness of ≈ 100 μm in the c -axis direction and the dimensions of 0.4×0.2 mm². The crystal axis were determined by x-ray analysis. Details of the growth method and the techniques used for characterization of the samples are given in Ref. 13.

The photoinduced (PI) reflection $\Delta R/R$ as a function of time at different temperatures is shown in Fig. 1 for the

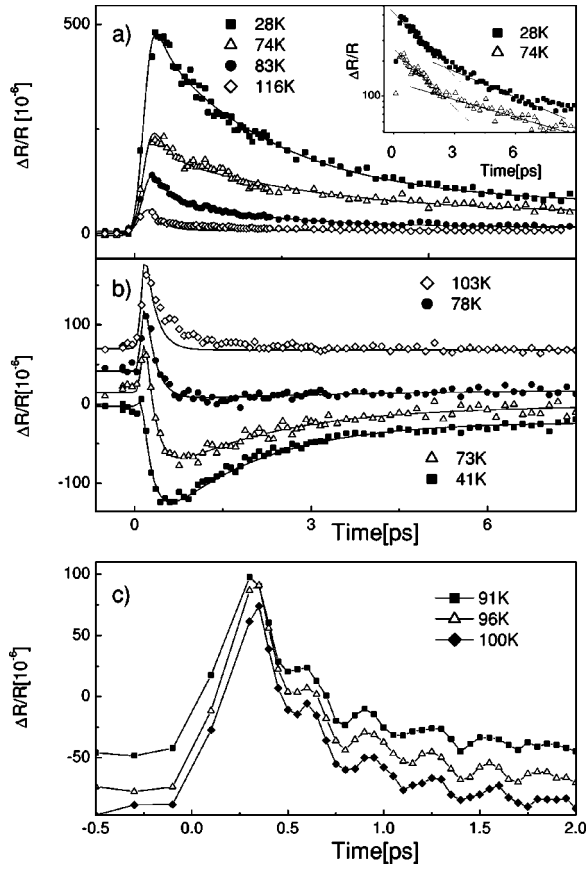


FIG. 1. The photoinduced reflection $\Delta R/R$ from $\text{YBa}_2\text{Cu}_4\text{O}_8$ at different temperatures above and below T_c as a function of time, measured (a) with the polarization of probe pulse in the direction parallel to the crystal axis a and (b) parallel to (the direction of chains) the crystal axis b . The inset shows the data at 28 K and 74 K already presented in (a) on the logarithmic scale, so that a two-component decay can be easily observed. In (c) we show weak oscillations of $\Delta R/R$ with frequency of $3.0(\pm 0.3)$ THz observed above T_c and attributed to a coherent phonon mode.

direction of polarization of probe pulse along a axis and b axis of Y124. The chains are parallel to the b axis and the PI response in these directions clearly shows a presence of at least two relaxation process with different signs of $\Delta R/R$. At temperatures $T > T_c$, we see a signal with a positive $\Delta R/R$ and with a relatively fast relaxation time ($\tau_p \approx 0.2$ ps). As the temperature is lowered below T_c , a second component with a longer relaxation time ($\tau_G \approx 2$ ps) and negative sign starts to appear. This kind of behavior of the two components is also present in PI response with the probe polarization along a axis, which can be clearly seen, if data are presented on a logarithmic scale as in the inset of Fig. 1. The relaxation of $\Delta R/R$ after 200 fs can be modeled with a function of the form $\Delta R(t, T)/R = G(T)\exp(-t/\tau_G) + P(T)\exp(-t/\tau_p)$, where the temperature-dependent amplitudes $G(T)$ [$G(T) = 0$ for $T \geq T_c$] and $P(T)$ can have the same or opposite sign below T_c , depending on the polarization direction of the probe pulse. Fits that are presented by a continuous line in Fig. 1 are in a good agreement with the data. We note that above T_c the data show a slight departure from a simple exponential

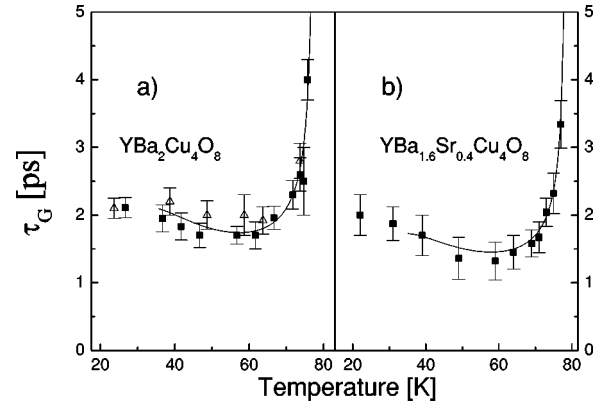


FIG. 2. The relaxation times τ_G as a function of temperature (a) for $\text{YBa}_2\text{Cu}_4\text{O}_8$, with the direction of polarization of probe pulse along a axis (open triangles) and b axis (squares), and (b) for $\text{YBa}_{1.6}\text{Sr}_{0.4}\text{Cu}_4\text{O}_8$ with the direction of polarization of probe pulse along b axis (squares).

decay. Similar behavior above T_c has also been reported in Ref. 5, where two components of opposite sign below T_c and one component slightly nonexponential above T_c were observed on $\text{Tl}_2\text{Ba}_2\text{Ca}_2\text{Cu}_3\text{O}_{10}$. Whether a stretch exponential decay is relevant or the presence of an additional component is the reason for the discrepancy, we cannot assert with a good degree of certainty from the present data.

In addition to the two picosecond components, a weak oscillatory component with frequency of $3.0(\pm 0.3)$ THz can also be seen above T_c . This is shown in Fig. 1(c). Such an oscillatory component of the same frequency was already observed with pump-probe measurements on Y124 at room temperature.¹⁴

We analyze the temperature dependences of relaxation time τ_G and of both amplitudes $G(T), P(T)$ in the same way as was done previously for Y123.¹ The temperature dependence of quasiparticle recombination time in a superconductor with a temperature-dependent gap $\Delta(T)$ below T_c is described by equation¹²

$$\tau_G = \frac{\hbar \omega_{ph}^2 \ln \left\{ \left(\frac{E_I}{2N(0)[\Delta(0)]^2} + e^{-\Delta(T)/k_B T} \right)^{-1} \right\}}{12\Gamma_{\omega_{ph}}[\Delta(T)]^2}, \quad (1)$$

where ω_{ph} is a typical phonon frequency, $N(0)$ is the density of states (DOS), Γ_{ω} is a characteristic phonon linewidth, and $\Delta(0)$ is the value of the gap at $T = 0$ K. In Fig. 2 we show divergent behavior near T_c in the temperature dependence of τ_G , predicted by Eq. (1) (solid curve). The data points were obtained from the fits of the time evolution of $\Delta R/R$ for Y124 along the a and b axes and for Y124:Sr along the b axis. In the fits we have used the following values of parameters in Eq. (1) $\omega_{ph} = 400 \text{ cm}^{-1}$, $\Gamma_{\omega} = 10 \text{ cm}^{-1}$, $N(0) = 5 \text{ eV}^{-1} \text{ cell}^{-1} \text{ spin}^{-1}$, and a BCS functional form for the temperature-dependent gap $\Delta(T)$. The fitting parameter was $\Delta(0)$.

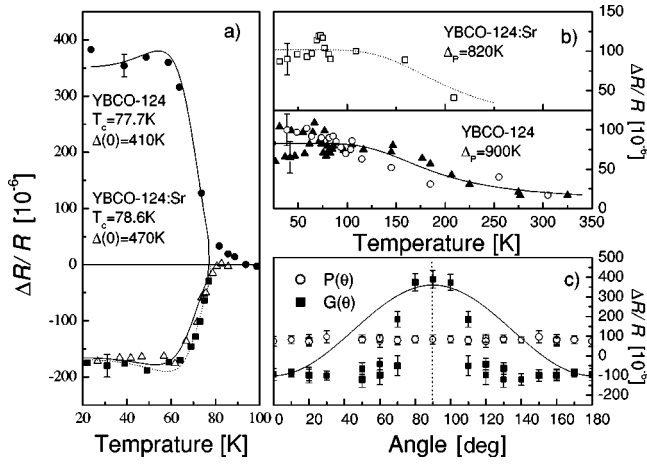


FIG. 3. (a) The temperature dependence of photoinduced amplitudes $G(T)$ for $\text{YBa}_2\text{Cu}_4\text{O}_8$, measured with the polarization of probe pulse along a axis (circles) and b axis (open triangles), and for $\text{YBa}_{1.6}\text{Sr}_{0.4}\text{Cu}_4\text{O}_8$ with the polarization along b axis (squares). The values of $\Delta(0)$ obtained from the fits are also shown. (b) The photoinduced amplitudes $P(T)$ for $\text{YBa}_2\text{Cu}_4\text{O}_8$ and $\text{YBa}_{1.6}\text{Sr}_{0.4}\text{Cu}_4\text{O}_8$ as a function of temperature, measured at the same polarizations as in (a). We also report on the obtained values of Δ_p . (c) The polarization dependence of photoinduced amplitudes $G(T=45\text{ K}, \theta)$ and $P(T=45\text{ K}, \theta)$ for $\text{YBa}_2\text{Cu}_4\text{O}_8$, together with the polarization dependence given by Eq. (6) (solid line).

In Fig. 3 we compare the measured temperature dependence of the signal amplitudes $G(T)$, $P(T)$ with those predicted by the theoretical expressions¹² for BCS temperature-dependent gap

$$G(T) = \frac{E_I / [\Delta(T) + k_B T/2]}{1 + \frac{2\nu}{N(0)\hbar\Omega_c} \sqrt{2k_B T / \pi \Delta(T)} \exp[-\Delta(T)/k_B T]} \quad (2)$$

and for temperature-independent gap

$$P(T) = \frac{E_I / \Delta_p}{1 + \frac{2\nu}{N(0)\hbar\Omega_c} \exp[-\Delta_p/k_B T]} \quad (3)$$

In the fits we used $\nu=18$ for the number of modes interacting with quasiparticles, $\Omega_c=0.1\text{ eV}$ for a typical phonon cutoff frequency and $N(0)=5\text{ eV}^{-1}\text{ cell}^{-1}\text{ spin}^{-1}$ for the DOS. The agreement between the data and the theory is seen to be very good.

In Fig. 3(c), we show a polarization dependence of both amplitudes $G(T, \theta)$ and $P(T, \theta)$ for Y124 at $T=45\text{ K}$. $P(T)$ does not show any polarization dependence, which was also confirmed by polarization measurements above T_c . In contrast, the polarization dependence of $G(T)$ shows a significant angular dependence, exhibiting a change of sign as the polarization direction is changed from parallel to perpendicular to the Cu-O chains.

This angular dependence can be understood in terms of the anisotropy of the probe transition matrix elements. We first note that in spite of the fact that Y124 is orthorhombic,

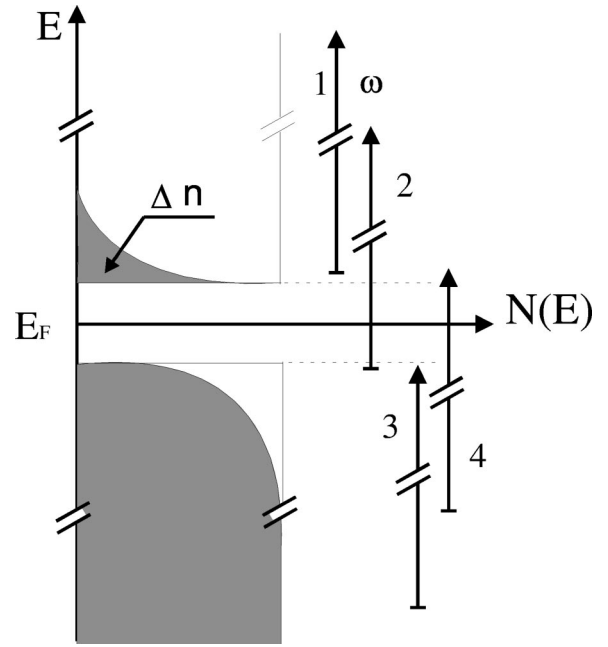


FIG. 4. The four possible transitions, which can give rise to a photoinduced probe signal arising from a change in quasiparticle population Δn . If the transition probabilities do not cancel a non-zero photoinduced reflectivity transient is observed. The polarization anisotropy of the probe signal arises due to the transitions having different probabilities in different directions relative to the crystal axes. Note, the scheme is drawn for $T=0\text{ K}$.

the main contribution to the probe signal comes from interband resonance transitions⁹ that involves atomic wave functions in which the dipolar matrix elements have a fourfold rotational symmetry around the c axis. Without specifying exactly which transitions are involved, we can write the absorption coefficient in terms of the Fermi-golden rule,

$$\alpha \propto \int d\epsilon N(\epsilon) N(\epsilon + \omega) |\mathbf{M}(\epsilon, \omega)|^2 f(\epsilon) [1 - f(\epsilon + \omega)].$$

Here, $N(\epsilon)$ is the density of electronic states, $f(\epsilon)$ is the distribution function for holes, $\hbar\omega$ is the energy of the probe photons and $\mathbf{M}(\epsilon, \omega)$ is the dipole matrix element for the transition. For small perturbations, ΔR is proportional to the photoinduced absorption $\Delta\alpha$, so:

$$\Delta R \propto \Delta\alpha \propto \int d\epsilon N(\epsilon) |\mathbf{M}(\epsilon, \omega)|^2 (f'(\epsilon) - f(\epsilon)), \quad (4)$$

where $f'(\epsilon)$ is the nonequilibrium distribution function of the charge carriers. The integral is taken in the vicinity of the Fermi energy E_F over the width of the resonance⁹ and we assumed for simplicity that $N(\epsilon + \Omega)$ is constant within the resonance width.

If $\mathbf{M}(\epsilon, \omega)$ is constant over the whole range of energies $-\hbar\omega < \epsilon - E_F < \hbar\omega$, then $\Delta R = \Delta\alpha = 0$ because of the conservation of particles. In other words, the photoinduced *increase* in absorption, due to probe transitions 1 (see Fig. 4) originating from the photoexcited electron states at $\epsilon - E_F \approx \Delta$ just above the gap to unoccupied hole states at $\epsilon - E_F$

$\sim\hbar\omega+\Delta$, exactly cancels the *decrease* in absorption due to transitions 2 originating from occupied electronic states at $\epsilon-E_F\lesssim-\Delta$ just below the gap to unoccupied states at $\epsilon-E_F\sim\hbar\omega-\Delta$. The same is true for the hole transitions 3 and 4 (see Fig. 4).

Turning to the situation in hand, we assume that $\mathbf{M}(\epsilon,\omega)$ is not constant and proceed to derive an expression for the polarization anisotropy of the probe absorption. The general expression for the square of the dipolar matrix element can be written as

$$|\mathbf{M}(\epsilon)|^2 = M_x^2(\epsilon)\sin^2(\theta) + M_y^2(\epsilon)\cos^2(\theta),$$

where θ is the angle between polarization of light and the b axis. For an orthorhombic structure $M_x \neq M_y$. On the other hand, the main contribution to M which comes from atomic wave functions is independent of θ , so we can expand M in the vicinity of the Fermi energy and express matrix element in the form

$$M_{x,y}(\epsilon) = M_0 + \gamma_{x,y}\epsilon, \quad (5)$$

where $\gamma_{x,y} = dM_{x,y}/d\epsilon$ and the derivative is taken at the Fermi energy. Substituting this expression into Eq. (4), we obtain a qualitative description of the angular dependence of the probe signal $G(\theta)$ and $P(\theta)$,

$$\Delta R \propto \Delta \alpha \propto M_0 [\gamma_x \sin^2(\theta) + \gamma_y \cos^2(\theta)] \Delta n. \quad (6)$$

Here, Δn is the number of photoexcited quasiparticles, as described in Ref. 12. The values of $\gamma_{x,y}$ can be doping dependent and can easily have different signs, depending strongly on ω and the material's band structure in the vicinity of the resonance $\epsilon - E_F \sim \hbar\omega \pm \Delta$. However, since the probe polarization anisotropy is a consequence of the anisotropy

of the probe transition matrix elements, Eq. (6) unfortunately does not give any direct information regarding the anisotropy of the low-energy electronic gap structure. In Fig. 3(c), we plot the polarization dependence of photoinduced reflectivity amplitude given by Eq. (6) using $\gamma_x/\gamma_y = 35/(-10)$, which is shown to describe the main features of the data quite well, despite the fact that Eq. (6) is based on the oversimplified expansion of the matrix elements [Eq. (5)]—neglecting higher-order terms.

An alternative model discussing carrier relaxation dynamics in HTSC has been recently proposed,¹⁵ whereby the main contribution to $\Delta R/R$ in the region at $\omega \sim 1.5$ eV comes from spectral weight transfer in the real part of the optical conductivity $\sigma(\omega)$ from $\omega=0$ to $\omega \approx \Delta$. Since $\Delta\sigma$ is always positive¹⁵ the sign of $\Delta R/R$ is determined by the real and imaginary part of the dielectric constant ϵ at $\omega \sim 1.5$ eV (Ref. 15). Using the published values of ϵ (Ref. 16), we find that the proposed model¹⁵ gives exactly the opposite sign of $\Delta R/R$ (as a function of probe polarization) as observed experimentally.

In conclusion, the femtosecond relaxation dynamics in Y124 is found to be very similar to that reported previously in Y123.¹ The results are also consistent with time-resolved terahertz spectroscopy measurements,¹⁷ which directly probed the recovery of the condensate after photoexcitation, both agreeing well with the model.¹² The observed probe polarization dependence and sign change of the transient signal below T_c is described well by a model that considers the anisotropy of the probe transition matrix elements in Y124, and is not directly related to the symmetry of the order parameter.

The authors would like to acknowledge A. Mironov of the Chemical Department, Moscow State University for single-crystal x-ray investigation of the samples.

¹J. Demsar *et al.*, Phys. Rev. Lett. **82**, 4918 (1999).

²D.C. Smith *et al.*, J. Low Temp. Phys. **117**, 1059 (1999).

³P. Gay *et al.*, J. Low Temp. Phys. **117**, 1025 (1999).

⁴J. Demsar *et al.*, Phys. Rev. B **63**, 054519 (2001).

⁵G.L. Eesley *et al.*, Phys. Rev. Lett. **65**, 3445 (1990).

⁶S.G. Han *et al.*, Phys. Rev. Lett. **65**, 2708 (1990).

⁷R.A. Kaindl *et al.*, Science **287**, 470 (2000).

⁸D.H. Reitze *et al.*, Phys. Rev. B **46**, 14309 (1992).

⁹C.J. Stevens *et al.*, Phys. Rev. Lett. **78**, 2212 (1997).

¹⁰P. Gay *et al.*, Physica C **341-348**, 2269 (2000).

¹¹D. Mihailovic and J. Demsar, in *Spectroscopy of Superconducting Materials*, edited by E. Faulques, ACS Symposium Series, Vol. 730 (ACS, Washington, 1999).

¹²V.V. Kabanov *et al.*, Phys. Rev. B **59**, 1497 (1999).

¹³J. Karpinski *et al.*, Phys. Rev. B **64**, 094518 (2001).

¹⁴O.V. Misochko, K. Sakai, and S. Nakashima, Physica C **329**, 12 (2000).

¹⁵G.P. Segre *et al.*, Phys. Rev. Lett. **88**, 137001 (2002).

¹⁶J. Kircher *et al.*, Phys. Rev. B **48**, 3993 (1993).

¹⁷R.D. Averitt *et al.*, Phys. Rev. B **63**, 140502 (2001).